

Published in final edited form as:

Arthritis Rheum. 2013 March ; 65(3): 660–670. doi:10.1002/art.37796.

Genetic and cellular evidence of decreased inflammation associated with reduced post-traumatic arthritis in MRL/MpJ mice

John S. Lewis Jr^{1,*}, Bridgette D. Furman^{1,*}, Evan Zeitler¹, Janet L. Huebner², Virginia B. Kraus², Farshid Guilak¹, and Steven A. Olson¹

Steven A. Olson: olson016@mc.duke.edu

¹Department of Orthopaedic Surgery, Duke University Medical Center, Durham, NC 27710

²Department of Medicine, Duke University Medical Center, Durham, NC 27710

Abstract

Objective—To examine the relationship between inflammation and post-traumatic arthritis in a murine intra-articular fracture model.

Methods—Male C57BL/6 and MRL/MpJ “superhealer” mice received tibial plateau fractures using a previously established method. Mice were sacrificed at 0 (within 4 hours), 1, 3, 5, 7, 28 and 56 days after fracture. Synovial tissue samples were taken prior to fracture and at 0, 1, 3, 5 and 7 days to examine gene expression of pro-inflammatory cytokines using RT-PCR. Synovial fluid and serum samples were collected to measure cytokine concentrations using ELISA. Histologic analysis was used to evaluate whole joint synovitis and cartilage degradation, and immunohistochemistry to evaluate the distribution of interleukin-1 in the joint tissues from all time points.

Results—Compared to the C57BL/6 mice, the MRL/MpJ mice had lower intra-articular and systemic inflammation following joint injury, as evidenced by lower gene expression of TNF- α and IL-1 β in synovial tissue, and lower protein levels of IL-1 α and IL-1 β in the synovial fluid, serum, and joint tissues. Furthermore, MRL/MpJ mice had lower gene expression of macrophage inflammatory proteins (MIPs) and macrophage derived chemokine (MDC/CCL22) in synovial tissue, and reduced acute and late-stage infiltration of synovial macrophages after joint injury.

Conclusion—C57BL/6 mice exhibited higher levels of inflammation than MRL/MpJ mice, which are protected from post-traumatic arthritis in this model. These data thus suggest an association between joint tissue inflammation and post-traumatic arthritis in mice.

Keywords

cartilage; osteoarthritis; trauma; injury; intra-articular fracture; synovium; inflammation; chemokine

Joint trauma resulting in post-traumatic arthritis (PTA) is estimated to account for 12% of the 27 million Americans with symptomatic osteoarthritis (OA) (1–3). Even with optimal treatment, displaced articular fractures in the lower extremity have a 10–20% incidence of

Corresponding author: Steven A. Olson, M.D., Duke University Medical Center, Box 3389, Durham, NC 27710, Tel (919) 668-3000, Fax (919) 668-2933.

*These authors contributed equally to this manuscript and share first authorship.

PTA (4). Despite the impact of PTA, the sequence of events leading to arthritis following an articular fracture is not fully understood.

An articular fracture is a complex event with several injurious aspects, including mechanical insult to the joint tissues, release of blood and marrow contents into the joint space, and potentially systemic polytrauma (5). The inflammatory response resulting from articular fracture may be a significant factor in the progression of PTA, but its effect remains incompletely characterized (6). Pro-inflammatory cytokines such as interleukin-1 (IL-1) and tumor necrosis factor- α (TNF- α) are up-regulated in injured and degenerative joints and may play an important role in the pathogenesis of PTA similar to their role in primary OA of joints in patients without antecedent injury (7, 8). The manner in which these cytokines and mediators influence sustained joint tissue inflammation and cartilage degeneration following articular trauma, however, remains unclear.

In order to further characterize these mechanisms, we developed a murine model of articular fracture of the tibial plateau that results in progressive arthritic changes in the bone, articular cartilage, and other joint tissues in the C57BL/6 mouse (9). However, the inbred MRL/MpJ strain, known as the “*superhealer*”, is protected from PTA and does not develop degenerative joint changes following articular fracture (10). The MRL/MpJ strain is of particular interest due to its demonstrated ability to regenerate a wide array of tissues ranging from fibrocartilage in the ear to myocardium to articular cartilage (11–14). While the exact genetic differences responsible for the enhanced regenerative capability of this strain are not known, the MRL/MpJ mouse exhibits decreased levels of inducible pro-inflammatory cytokines such as IL-1 and TNF- α in response to lipopolysaccharide (LPS) stimulation (15).

We hypothesized that the ‘*superhealer*’ MRL/MpJ strain of mice responds to closed articular fracture with a reduced inflammatory response compared to C57BL/6 mice. We measured synovial gene expression of inflammatory cytokines and chemokines, synovial fluid and serum levels of inflammatory cytokines, and the extent of infiltrating inflammatory cells in the synovium, at a variety of early and late time points in MRL/MpJ mice compared to C57BL/6 mice following closed articular fracture.

MATERIALS AND METHODS

All procedures were performed in accordance with an IACUC-approved protocol. Male C57BL/6 (n=42; Charles River Laboratories) and male MRL/MpJ (n=42; The Jackson Laboratory) mice were obtained at 8 weeks of age and housed until 16 weeks of age, which represents the age of peak bone mass (16). At this point, 6 mice from each strain were sacrificed as pre-fracture controls. All experimental mice received moderate closed articular fractures of the left lateral tibial plateau. Animals were anesthetized and placed in a custom cradle with the left hind limb in 90° of flexion. As previously described (9), a custom indenter was attached to a materials testing system (ElectroForce ELF3200, Bose Corp., Minnetonka MN) and applied a 10N compressive pre-load to the anterior aspect of the proximal tibial plateau of the left hind limb. The tibia was then loaded in compression at a rate of 20 N/s in load-control mode to induce fracture. The total displacement of the indenter was scaled to the relative size of the tibial plateau in the mice strains (2.5mm for C57BL/6; 3.2 mm for MRL/MpJ), which we have shown results in equivalent injury severity (10). High-resolution digital radiographs were obtained to confirm fracture (MX-20, Faxitron, Lincolnshire, IL). The right non-fractured hind limb was used as a contralateral control. No immobilization or surgical intervention was employed. Animals were allowed immediate full weight-bearing.

For each strain, 6 mice were sacrificed at 0, 1, 3, 5, 7, 28, and 56 days post-fracture. At pre-fracture, 0 (within four hours of fracture), 1, 3, 5, and 7 days post-fracture, the following samples were obtained after sacrifice: serum was collected via retro-orbital bleed followed by cardiac stick; synovial fluid was collected from both knees from each animal using a calcium sodium alginate compound as previously described (17); and joint capsule tissue was obtained for RNA isolation from both knees. At pre-fracture, 0, 1, 3, 5, 7, 28, and 56 days post-fracture, both hind limbs of all animals were formalin-fixed and paraffin-embedded for histology and immunohistochemistry (IHC).

Gene expression was measured in synovium from joint capsule tissue harvested with a 3 mm biopsy punch as previously described (18). Tissue was pooled for each knee from 6 animals at 0, 1, 3, 5, and 7 days post-fracture. RNA was isolated using a two-step Trizol protocol. RT-PCR was run on 1µg of RNA in duplicate using SYBR Green Master Mix and the commercially-available RT² Profiler PCR array for mouse inflammatory cytokines and receptors for 84 genes (SABiosciences, Frederick, MD). Relative mRNA for each gene of each sample was first normalized to the geometric mean of three housekeeping genes (GAPDH, HPRT1, and HSP90ab1) in that sample and then compared to mRNA expression prior to fracture using the $2^{-\Delta\Delta CT}$ method (19). In accordance with commercial analysis software provided by the manufacturer, results were considered significant when mRNA expression levels were 3-fold different than that of pre-fracture mice.

Concentrations of IL-1α, IL-1β, and TNF-α were measured in synovial fluid and serum samples using commercially-available ELISA kits (MLA00; MLB00B; and MTA00B; R&D Systems) and run as directed by the manufacturer with the following exceptions: (a) the two-fold dilution series of the standard was extended to more accurately quantify samples containing protein levels between 0 and 7.8 pg/mL; and (b) the assay required a 1:5 dilution of the synovial fluid samples and 50µL of neat serum.

Both hind limbs from each animal at all time points were placed in 10% neutral buffered formalin for 72 hours. The limbs were then decalcified (Cal-Ex Decalcification Solution, Fisher Scientific) for 72 hours, dehydrated in ethanol, infiltrated with xylene, and paraffin-embedded using a commercially-available automated tissue processor (ASP300S, Leica Microsystems).

Immunohistochemistry was used to localize IL-1α and IL-1β cytokine proteins within the joint tissue. Serial sections (8µm) of fixed limbs from both strains at all time points were pre-treated by heating the tissue for 20 minutes at 95°C for antigen retrieval. Endogenous peroxidase was quenched with 3% H₂O₂ in methanol with 0.1% w/v saponin for membrane permeabilization for 45 minutes in the dark. Sections were then stained with a polyclonal antibody against murine IL-1β (anti-mouse IL-1β/IL-1F2, AF-401-NA, R&D Systems) or murine IL-1α (anti-mouse IL-1α, AF-400-NA, R&D Systems) at 1:10 dilution at room temperature for 18 hours. During every staining protocol, negative controls were created simultaneously by application of 1–2% horse blocking serum to tissue sections instead of the primary antibody. Chromogenic detection was achieved with DAB substrate (Vectastain) and sections were digitally photographed. Regions of the joint evaluated included the articular cartilage, calcified cartilage, subchondral bone, and synovium. Intensity of positive staining for cytokines was assessed qualitatively using a discrete four-point scoring system.

Synovitis was assessed using histologic analysis and semi-quantitative grading. Serial sections (8µm) of fixed limbs from both strains at all time points were stained with standard Harris hematoxylin and eosin (H&E), and digital images of the joints were obtained. All limbs were evaluated at the synovial insertion of the lateral tibia, lateral femur, medial tibia, and medial femur using a modified form of an established standardized synovitis score (20,

21) for a total possible site score of 0 to 6. The average from four independent blinded graders was reported for each limb. The score of all four sites was summed for a total joint synovitis score.

Immunohistochemistry was used to assess synovial infiltration of activated macrophages. Serial sections (8µm) of fixed limbs from both strains at all time points were pre-treated with 0.05% Proteinase K (Sigma-Aldrich) for 5 minutes at 37°C for antigen retrieval as previously described (22). Endogenous peroxidase was quenched with 3% H₂O₂ in methanol for 30 minutes. Sections were stained with a monoclonal antibody against a surface marker of activated macrophages (anti-F4/80, Clone CI:A3-1, Serotec) at 1:100 dilution at room temperature for 1 hour. During every staining protocol, negative controls were created simultaneously by application of 1–2% rabbit blocking serum to tissue sections instead of the primary antibody. Chromogenic detection was achieved with DAB substrate (Vectastain) and digital images of the joint tissue were obtained.

All statistical analyses were performed using Statistica 7 software (StatSoft). Non-parametric statistical analyses were utilized with significance reported at the 95% confidence level. For serum levels of cytokines, the Mann-Whitney U test was used to compare differences between C57BL/6 and MRL/MpJ strains at each time point, and the Kruskal-Wallis test was used to compare differences with the baseline pre-fracture condition and time post-fracture within a mouse strain. For synovial fluid levels of cytokines and joint synovitis scores, the Wilcoxon matched pairs test was used to compare differences between fractured and non-fractured limbs at each time point for C57BL/6 and MRL/MpJ strains independently. The Mann-Whitney U test was used to compare difference between C57BL/6 and MRL/MpJ strains at each time point for fractured and non-fractured limbs independently, and the Kruskal-Wallis test was used to compare differences with the baseline pre-fracture condition and time post-fracture within a mouse strain.

RESULTS

Gene expression of inflammatory cytokines and chemokines

For C57BL/6 mice, 54 of 84 inflammatory cytokine and receptor genes evaluated by RT-PCR were up-regulated in the synovial tissue after lateral plateau fracture, and 0 of 84 genes were down-regulated. In contrast, for MRL/MpJ mice, only 33 of 84 inflammatory genes evaluated were up-regulated in the synovial tissue after lateral plateau fracture, and 7 of 84 genes were down-regulated.

Several genes of interest were highly up-regulated after fracture. TNF-α gene expression in C57BL/6 mice was significantly up-regulated at day 1 (13-fold) and remained significantly elevated through day 7 after fracture (Figure 1A). In contrast, MRL/MpJ mice showed no significant increase in TNF-α gene expression (less than 1.5-fold) in synovial tissue after fracture at any time point.

IL-1α gene expression was up-regulated after fracture for both strains (Figure 1A). In C57BL/6 mice, IL-1α gene expression was significantly up-regulated at 1 day after fracture (7-fold) and remained significantly elevated through day 5 before returning to baseline levels at day 7 (Figure 1A). In MRL/MpJ mice, IL-1α gene expression was intermittently up-regulated at day 0 (7-fold), day 3 (4-fold) and day 7 (3-fold) after fracture.

IL-1β gene expression was up-regulated after fracture to much higher levels than IL-1α (Figure 1A). In C57BL/6 mice, IL-1β gene expression was up-regulated 720-fold at day 0, within 4 hours of fracture, compared to a 74-fold increase in MRL/MpJ mice (Figure 1A). Furthermore, IL-1β gene expression remained over 200-fold elevated in C57BL/6 mice at 1

and 3 days post fracture, with significant elevation extending to days 5 and 7 post-fracture. In contrast, IL-1 β gene expression in MRL/MpJ mice returned to pre-fracture levels at day 3.

Systemic and local protein levels of IL-1 α , IL-1 β , and TNF- α

Serum IL-1 α was significantly increased following fracture for both C57BL/6 and MRL/MpJ mice. For C57BL/6 mice, peak concentrations of serum IL-1 α occurred at days 1 and 3 post-fracture compared to pre-fracture ($p < 0.05$). For MRL/MpJ mice, IL-1 α concentrations at day 0 and 7 post-fracture were significantly elevated compared to pre-fracture levels ($p < 0.05$, Figure 1B). The effect of strain was found to be significant, as C57BL/6 mice showed significantly higher total serum concentrations of IL-1 α than MRL/MpJ mice ($p < 0.0001$) mice at days 1 and 3 post-fracture ($p < 0.05$, Figure 1B). It should be noted that for 22 of 72 C57BL/6 and 24 of 72 MRL/MpJ synovial fluid samples, the IL-1 α protein concentration was below the detection limit of the immunoassay. The distribution of samples below the detection limit was concentrated at pre-fracture and days 0, 1, and 7 post-fracture in both mouse strains and were similarly distributed between right and left limbs. These samples were assigned half the lower limit of detection of the assay for statistical analyses.

Serum IL-1 β was also increased following fracture for both C57BL/6 and MRL/MpJ mice with higher concentrations in C57BL/6 mice compared with the MRL/MpJ mice ($p < 0.001$). C57BL/6 mice had significantly higher levels of IL-1 β compared to MRL/MpJ mice at pre-fracture, 1, 3 and 5 days after fracture. The highest concentrations of IL-1 β in both strains occurred in serum on day 1 post-fracture (Figure 1C). The elevation in serum concentrations of IL-1 β at day 1 was significantly higher than at pre-fracture, day 5, and 7 for C57BL/6 mice and significantly higher than at pre-fracture and day 3 for MRL/MpJ mice ($p < 0.05$, Figure 1C).

TNF- α was undetectable in the majority of synovial fluid samples analyzed (47 of 72 C57BL/6 and 43 of 72 MRL/MpJ). Among the samples with sufficient protein concentrations to analyze, no effect of strain or time on synovial fluid TNF- α was observed (Figure 2). Given that protein concentrations were expected to be higher in the synovial fluid than in the systemic serum, subsequent analysis of serum levels of TNF- α was not performed.

IL-1 α protein concentrations in synovial fluid for both C57BL/6 and MRL/MpJ mice strains showed non-significant increases on days 3 and 5 post-fracture in both fractured and contralateral (non-fractured) limbs (Figure 2). Interestingly, concentrations of IL-1 α in the synovial fluid were not different in fractured and non-fractured limbs in either strain at any time point. These data in combination with serum levels suggest a systemic response of IL-1 α following articular fracture.

IL-1 β protein concentration in the synovial fluid of fractured limbs for both C57BL/6 mice and MRL/MpJ mice was significantly elevated compared to the concentration in the non-fractured limb at 0 to 7 days after fracture ($p < 0.05$; Figure 2). Peak concentrations of IL-1 β for both strains were comparable and occurred at day 0 (i.e., within four hours of fracture). Interestingly, baseline and non-fractured limb synovial fluid levels of IL-1 β were significantly higher in MRL/MpJ mice compared to C57BL/6 mice. However, the fold change was greater in the C57BL/6 mice post-fracture. C57BL/6 mice showed a 7-fold increase in IL-1 β concentration in the synovial fluid of the fractured limb relative to the non-fractured limb, while MRL/MpJ mice showed only a 2-fold increase. Taken together these data suggest a local intra-articular response of IL-1 β in synovial fluid after articular fracture followed by a systemic increase in serum levels.

IL-1 α and IL-1 β protein expression in joint tissues

Distribution of both isoforms of IL-1 in various joint tissues was assessed via immunohistochemistry. Regions of the joint evaluated included the articular cartilage, calcified cartilage, subchondral bone, and synovium (Figure 3A). For C57BL/6 fractured limbs, there was a peak in IL-1 α by IHC staining in the articular cartilage, calcified cartilage, and synovium at day 1 post-fracture (Figure 3B). For C57BL/6 non-fractured limbs, there was a peak in IL-1 α staining in the same three joint tissues (articular cartilage, calcified cartilage, and synovium) at 3 days post-fracture. For MRL/MpJ fractured limbs, there was an increase in IL-1 α staining in the synovium only at days 1 and 7 post-fracture (Figure 3B). For MRL/MpJ non-fractured limbs, there was minimal variation in IL-1 α in joint tissue in any region of the joint at any time point.

For C57BL/6 fractured limbs, there was a peak in IL-1 β identified by IHC staining in both the subchondral bone and synovial tissue at day 3 after fracture (Figure 3C). For C57BL/6 non-fractured limbs, there was a peak in IL-1 β staining in the synovium only at day 3 post-fracture. For MRL/MpJ fractured limbs, there was a peak in IL-1 β staining in the synovium only at day 3 post-fracture (Figure 3C). For MRL/MpJ non-fractured limbs, there was no significant change in IL-1 β in joint tissue in at any region of the joint at any time point.

Synovial inflammation following fracture

Grading of the synovium using a modified synovitis score revealed no significant effect of strain at any of the time points examined (mean synovitis score \pm SD). Synovitis progressed similarly in both strains until day 7, when C57BL/6 mice (12.8 ± 3.7) showed a significant elevation from pre-fracture samples (2.0 ± 3.1 , $p < 0.05$), while MRL/MpJ mice (10.8 ± 2.8) demonstrated a non-significant elevation from pre-fracture samples (3.7 ± 1.5). At 28 and 56 days post-fracture, synovitis decreased in both, returning to near pre-fracture levels for C57BL/6 (3.7 ± 0.7) and MRL/MpJ (3.7 ± 2.9) mice.

Gene expression of macrophage chemokines

Gene expression of multiple proteins associated with macrophage chemoattraction was up-regulated following fracture in both strains, but less so in MRL/MpJ mice (Figure 4). CCL3 (macrophage inflammatory protein -1, MIP-1 α) and CCL4 (MIP-1 β) expression were significantly elevated in both strains on all days tested, although more so in C57BL/6 mice than MRL/MpJ mice. CCL3 expression peaked in both strains on day 3 after fracture, with a 274-fold increase in C57BL/6 mice and only a 42-fold increase in the MRL/MpJ strain. CCL4 expression peaked on day 3 after fracture with a 140-fold increase in C57BL/6 mice and only a 36-fold increase in MRL/MpJ mice. CCL9 (MIP-1 γ) exhibited significant increases in gene expression in both strains on days 0 through 5, and in C57BL/6 mice on day 7 as well (Figure 4). CCL9 expression peaked on day 1 with a 25-fold increase in C57BL/6 mice and only an 8-fold peak increase on day 0 in MRL/MpJ mice. CCL20 (MIP-3 α) gene expression was significantly elevated in C57BL/6 mice on days 1, 3 and 5, peaking on day 5 (12-fold increase); MRL/MpJ mice showed elevated gene expression on days 1 and 5, with a peak on day 1 (35-fold increase). CCL19 (MIP-3 β) expression was significantly elevated in C57BL/6 mice on all days tested, but not significant on any day for MRL/MpJ mice. CCL22 (or macrophage derived chemokine, MDC) gene expression was elevated following fracture (Figure 4) as well. Significant changes were seen in both strains on days 0, 3, 5 and 7 after fracture. The peak occurred for both strains on day 7, with a 27-fold change in C57BL/6 mice and only a 6-fold change in MRL/MpJ mice.

Acute and late-stage synovial infiltration of activated macrophages

Immunohistochemistry was used to identify activated macrophages present within the synovial tissue. Starting at day 3 post-fracture, C57BL/6 mice showed markedly increased infiltration of activated macrophages in the lateral synovial tissue of fractured joints compared to MRL/MpJ mice (Figure 5A). Furthermore, starting at day 3 post-fracture, C57BL/6 mice showed increased macrophage infiltration in the medial synovium, distant from the lateral fracture site, compared to MRL/MpJ mice (images not shown).

Joint sections from mice sacrificed at 28 and 56 days post-fracture were also examined. At these time points, C57BL/6 mice showed sustained inflammation in the lateral synovial tissue evidenced by persistent infiltration by activated macrophages (Figure 5B). In contrast, at these time points MRL/MpJ mice demonstrated a paucity of macrophages. Finally, C57BL/6 mice showed sustained global synovitis and joint-wide inflammation evidenced by persistent macrophage infiltration in the medial joint tissue whereas the MRL/MpJ mice showed minimal macrophage infiltration in the medial aspect of the joint at these later time points (images not shown).

DISCUSSION

Within four hours of fracture, MRL/MpJ mice showed decreased evidence of local intra-articular and systemic inflammation compared to C57BL/6 mice, and this attenuated inflammatory response may help explain how MRL/MpJ mice are protected from the development of PTA after articular fracture in our model (10). The findings of this study support the hypothesis that MRL/MpJ mice exhibit a significantly diminished inflammatory response following closed articular fracture compared to C57BL/6 mice. This observation suggests that inhibition of the inflammatory response after acute fracture may provide a novel therapeutic approach for PTA.

A number of modalities were employed to assess local and systemic inflammation after articular fracture. RT-PCR analysis was used to evaluate inflammatory gene expression, particularly that of IL-1 α , IL-1 β , TNF- α , and a variety of associated chemokines in synovial joint tissue to assess changes in inflammatory response to injury in the C57BL/6 compared to the MRL/MpJ strain. Serum and synovial levels of these pro-inflammatory cytokines were assessed as well. Specifically, IL-1 β was differentially elevated in the synovial fluid, serum, and synovium (by gene expression and IHC) while IL-1 α was elevated in serum and synovium (by gene expression and IHC). These data suggest a very early inflammatory response to articular fracture that is greater in the C57BL/6 strain than the MRL/MpJ strain.

The total synovial cellular infiltration following articular fracture was not different between the two strains. However, the C57BL/6 had significantly more activated macrophages in the synovium acutely, and this was sustained over time following articular fracture. By immunohistochemistry, IL-1 β was increased in the synovium and subchondral bone of the C57BL/6 strain and in the synovium of the MRL/MpJ strain. IL-1 α was increased in the synovium, cartilage, and calcified cartilage in the C57BL/6 strain while no increases were observed in the MRL/MpJ strain. These trends in IL-1 α staining are consistent with increases in synovial fluid protein levels in both limbs, and the increased serum levels followed by increased local protein expression in joint tissues from both limbs suggests a systemic response of IL-1 α following articular fracture. Articular fracture led to increased inflammatory gene expression in the synovium and inflammatory protein expression in the synovium, serum and synovial fluid, and subsequent activated macrophage infiltration of the synovium in association with progression to arthritis. Taken together, these findings suggest both a systemic response and a local intra-articular organ-level response of the joint to injury.

TNF- α levels did not increase in synovial fluid, although there was evidence of increased gene expression in the C57BL/6. It is possible this reflects the very short half-life of TNF- α , or binding of a significant amount available TNF- α that led to such a low level of detection in synovial fluid. TNF- α is the primary agent in pathophysiology of inflammatory arthritis, although is generally increased transiently and may rapidly return to undetectable levels *in vivo* (23). Other methods of selective inhibition of TNF- α may be needed to assess its role in PTA in this model.

Many chemokines are implicated in the pathogenesis of arthritis because of their increased expression levels in the synovial fluid of RA patients and in animal models (24–36). The proposed function of chemokines in arthritis development is through the regulation of inflammation, including infiltration of monocytes, macrophages, neutrophils and lymphocytes, among others (37, 38), but their exact contributions have not been fully elucidated. Synovial inflammation associated with arthritis and joint injury is likely driven in part by upregulation of chemokines and infiltration of inflammatory cells. The mediators and targets in the cascade of cytokine and chemokine upregulation is unclear, but previous studies of isolated synovial fibroblasts demonstrate that IL-1 and TNF- α upregulate the macrophage inflammatory protein chemokines CCL3, CCL4, CCL19, and CCL20 (32, 34, 35, 39–41). Our data also suggests that IL-1 and TNF- α are upregulated first with the highest levels observed within 1 day of injury, then with maximal upregulation of the macrophage inflammatory protein chemokines from 1 to 3 days post-injury, and followed by the simultaneous upregulation of the macrophage derived chemokine (CCL22) and infiltration of macrophages in the synovial tissue occurring 5 to 7 days post-injury (Figure 6). Furthermore, increased chemokine gene expression has been observed clinically in the synovium of patients undergoing surgery for meniscal injury, where synovial inflammation has been linked to increased pain and dysfunction (42).

The fracture in this model is displaced at the time of injury, and there is no attempt to treat the fracture, similar to other animal models of joint instability or injury (43, 44). The scale of the murine knee limits the possibilities of surgical reduction and fixation. An additional limitation of mouse models is the limited yield of biosamples, particularly from joint tissues. Pooling of tissue samples for RNA isolation in small animal models has been previously reported when specific joint tissues are of interest, such as the synovium and joint capsule tissue (18, 45, 46). An alternative strategy for isolating RNA from individual mice is to homogenize entire knee joints or paws, but this approach involves significant heterogeneity in the tissue sample (47–49). In spite of this limitation, we demonstrated that protein expression patterns in the synovial fluid and joint tissues in individual animals followed the same trends as the changes in mRNA levels from pooled samples.

The primary clinical analogy of this work is the early events after fracture in humans. To date, there is little data available characterizing the acute local and systemic response to articular fracture in humans. Future studies may examine the local and systemic cytokines and chemokines in patients with articular fracture. The time from fracture to reduction and fixation in a human joint can vary from less to 24 hours to longer than 3 weeks; the events that occur after fracture are potentially important in the subsequent response to injury. The pronounced infiltration of synovial macrophages observed in C57BL/6 mice starting at 3 days and continuing to 4 and 8 weeks post-fracture is characteristically seen in chronic inflammatory arthropathies such as rheumatoid arthritis. It is widely accepted that both inflammatory and destructive features of RA are driven through synovitis (50).

These findings suggest that inhibition of the inflammatory response may provide a novel therapeutic approach for PTA after articular fracture. Targeted blocking of specific cytokines has been the focus of several therapies for rheumatoid arthritis. This has led to the

development of specific inhibitors of TNF- α such as etanercept, a soluble form of TNF- α receptor II, and of IL-1 such as anakinra, a recombinant form of IL-1 receptor antagonist (IL-1Ra). Endogenous IL-1Ra is a specific receptor antagonist that competitively inhibits the binding of both IL-1 α and IL-1 β to their active receptor (51). Previous research has shown that administration of either TNF- α inhibitors (52–54) or IL-1Ra (55) in mouse models of collagen-induced arthritis ameliorate joint inflammation and cartilage destruction. Given the findings of the current study, future studies are warranted to better characterize the inflammatory response to articular injury in humans and to test, in animals and humans, anti-inflammatory agents for their ability to block the injury-related inflammatory response and the development of PTA.

In summary, MRL/MpJ mice had lower intra-articular and systemic inflammation following joint injury compared to C57BL/6 mice, as evidenced by lower gene expression of TNF- α and IL-1 β in synovial tissue and lower protein levels of IL-1 α and IL-1 β in the synovial fluid, serum, and joint tissues. Furthermore, C57BL/6 mice had increased gene expression of macrophage inflammatory proteins and macrophage derived chemokine in synovial tissue, and reduced acute and late-stage synovial macrophages after joint injury. Collectively, these data suggest an association between an increased and prolonged inflammatory response to articular fracture and PTA in mice. These results provide a basis for novel pharmacological approaches to targeting early inflammation of joint tissues following injury, which may halt the progression of post-traumatic arthritis.

Supplementary Material

Refer to Web version on PubMed Central for supplementary material.

Acknowledgments

We would like to thank Steve Johnson for his excellent technical support, and Drs. Amy McNulty and Beverley Fermor for their assistance. This study was supported by a Howard Hughes Medical Fellowship, the Arthritis Foundation, and NIH grants AR50245, AG15768, AR48182, and AR48852.

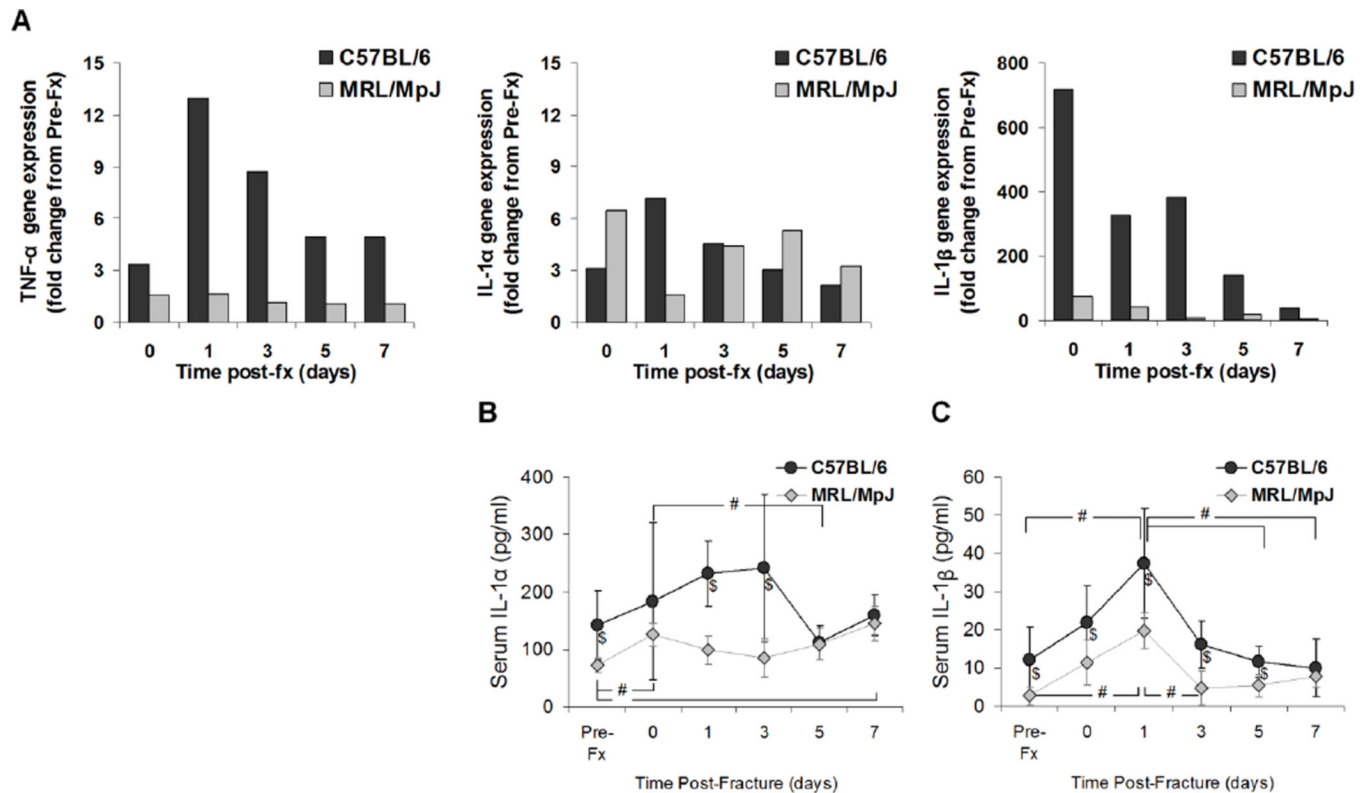
REFERENCES

1. Swiontkowski MF, Chapman JR. Cost and effectiveness issues in care of injured patients. *Clin Orthop Relat Res*. 1995; 318:17–24. [PubMed: 7671513]
2. Brown TD, Johnston RC, Saltzman CL, Marsh JL, Buckwalter JA. Posttraumatic osteoarthritis: a first estimate of incidence, prevalence, and burden of disease. *J Orthop Trauma*. 2006; 20(10):739–744. [PubMed: 17106388]
3. Lawrence RC, Felson DT, Helmick CG, Arnold LM, Choi H, Deyo RA, et al. Estimates of the prevalence of arthritis and other rheumatic conditions in the United States. Part II. *Arthritis Rheum*. 2008; 58(1):26–35. [PubMed: 18163497]
4. Matta JM. Fractures of the acetabulum: accuracy of reduction and clinical results in patients managed operatively within three weeks after the injury. *J Bone Joint Surg Am*. 1996; 78(11):1632–1645. [PubMed: 8934477]
5. Furman BD, Olson SA, Guilak F. The development of posttraumatic arthritis after articular fracture. *J Orthop Trauma*. 2006; 20(10):719–725. [PubMed: 17106385]
6. Guilak F, Fermor B, Keefe FJ, Kraus VB, Olson SA, Pisetsky DS, et al. The role of biomechanics and inflammation in cartilage injury and repair. *Clin Orthop Relat Res*. 2004; (423):17–26. [PubMed: 15232421]
7. Goldring MB. Osteoarthritis and cartilage: the role of cytokines. *Curr Rheumatol Rep*. 2000; 2(6): 459–465. [PubMed: 11123098]
8. Fernandes J, Martel-Pelletier J, Pelletier J. The role of cytokines in osteoarthritis pathophysiology. *Biorheology*. 2002; 39(1–2):237. [PubMed: 12082286]

9. Furman BD, Strand J, Hembree WC, Ward BD, Guilak F, Olson SA. Joint degeneration following closed intraarticular fracture in the mouse knee: a model of posttraumatic arthritis. *J Orthop Res*. 2007; 25(5):578–592. [PubMed: 17266145]
10. Ward BD, Furman BD, Huebner JL, Kraus VB, Guilak F, Olson SA. Absence of posttraumatic arthritis following intraarticular fracture in the MRL/MpJ mouse. *Arthritis Rheum*. 2008; 58(3): 744–753. [PubMed: 18311808]
11. Li X, Mohan S, Gu W, Miyakoshi N, Baylink DJ. Differential protein profile in the ear-punched tissue of regeneration and non-regeneration strains of mice: a novel approach to explore the candidate genes for soft-tissue regeneration. *Biochimica et Biophysica Acta (BBA) - General Subjects*. 2000; 1524(2–3):102–109.
12. Li X, Mohan S, Gu W, Baylink DJ. Analysis of gene expression in the wound repair/regeneration process. *Mammalian Genome*. 2001; 12:52–59. [PubMed: 11178744]
13. Leferovich JM, Bedelbaeva K, Samulewicz S, Zhang X-M, Zwas D, Lankford EB, et al. Heart regeneration in adult MRL mice. *PNAS*. 2001; 98(17):9830–9835. [PubMed: 11493713]
14. Fitzgerald J, Rich C, Burkhardt D, Allen J, Herzka AS, Little CB. Evidence for articular cartilage regeneration in MRL/MpJ mice. *Osteoarthritis Cartilage*. 2008; 16(11):1319–1326. [PubMed: 18455447]
15. Kench JA, Russell DM, Fadok VA, Young SK, Worthen GS, Jones-Carson J, et al. Aberrant wound healing and TGF-beta production in the autoimmune-prone MRL/+ mouse. *Clin Immunol*. 1999; 92(3):300–310. [PubMed: 10479535]
16. Beamer WG, Donahue LR, Rosen CJ, Baylink DJ. Genetic variability in adult bone density among inbred strains of mice. *Bone*. 1996; 18(5):397–403. [PubMed: 8739896]
17. Seifer DR, Furman BD, Guilak F, Olson SA, Brooks SC 3rd, Kraus VB. Novel synovial fluid recovery method allows for quantification of a marker of arthritis in mice. *Osteoarthritis Cartilage*. 2008; 16(12):1532–1538. [PubMed: 18538588]
18. Van Meurs JB, Van Lent PL, Joosten LA, Van der Kraan PM, Van den Berg WB. Quantification of mRNA levels in joint capsule and articular cartilage of the murine knee joint by RT-PCR: kinetics of stromelysin and IL-1 mRNA levels during arthritis. *Rheumatol Int*. 1997; 16(5):197–205. [PubMed: 9032819]
19. Livak KJ, Schmittgen TD. Analysis of relative gene expression data using real-time quantitative PCR and the 2(-Delta Delta C(T)) Method. *Methods*. 2001; 25(4):402–408. [PubMed: 11846609]
20. Krenn V, Morawietz L, Burmester GR, Kinne RW, Mueller-Ladner U, Muller B, et al. Synovitis score: discrimination between chronic low-grade and high-grade synovitis. *Histopathology*. 2006; 49(4):358–364. [PubMed: 16978198]
21. Lewis JS, Hembree WC, Furman BD, Tippets L, Cattel D, Huebner JL, et al. Acute joint pathology and synovial inflammation is associated with increased intra-articular fracture severity in the mouse knee. *Osteoarthritis Cartilage*. 2011; 19(7):864–873. [PubMed: 21619936]
22. Zwerina J, Redlich K, Polzer K, Joosten L, Kronke G, Distler J, et al. TNF-induced structural joint damage is mediated by IL-1. *PNAS*. 2007; 104(28):11742–11747. [PubMed: 17609389]
23. Gifford GE, Flick DA. Natural production and release of tumour necrosis factor. *Ciba Found Symp*. 1987; 131:3–20. [PubMed: 3131075]
24. Oppenheim JJ, Zachariae CO, Mukaida N, Matsushima K. Properties of the novel proinflammatory supergene "intercrine" cytokine family. *Annu Rev Immunol*. 1991; 9:617–648. [PubMed: 1910690]
25. Koch AE, Kunkel SL, Harlow LA, Johnson B, Evanoff HL, Haines GK, et al. Enhanced production of monocyte chemoattractant protein-1 in rheumatoid arthritis. *J Clin Invest*. 1992; 90(3):772–779. [PubMed: 1522232]
26. Taub DD, Oppenheim JJ. Chemokines, inflammation and the immune system. *Ther Immunol*. 1994; 1(4):229–246. [PubMed: 7584498]
27. Thornton S, Duwel LE, Boivin GP, Ma Y, Hirsch R. Association of the course of collagen-induced arthritis with distinct patterns of cytokine and chemokine messenger RNA expression. *Arthritis Rheum*. 1999; 42(6):1109–1118. [PubMed: 10366103]

28. Kasama T, Strieter RM, Lukacs NW, Lincoln PM, Burdick MD, Kunkel SL. Interleukin-10 expression and chemokine regulation during the evolution of murine type II collagen-induced arthritis. *J Clin Invest.* 1995; 95(6):2868–2876. [PubMed: 7769128]
29. Katrib A, Tak PP, Bertouch JV, Cuello C, McNeil HP, Smeets TJ, et al. Expression of chemokines and matrix metalloproteinases in early rheumatoid arthritis. *Rheumatology (Oxford).* 2001; 40(9): 988–994. [PubMed: 11561108]
30. Robinson E, Keystone EC, Schall TJ, Gillett N, Fish EN. Chemokine expression in rheumatoid arthritis (RA): evidence of RANTES and macrophage inflammatory protein (MIP)-1 beta production by synovial T cells. *Clin Exp Immunol.* 1995; 101(3):398–407. [PubMed: 7545093]
31. Shen PC, Wu CL, Jou IM, Lee CH, Juan HY, Lee PJ, et al. T helper cells promote disease progression of osteoarthritis by inducing macrophage inflammatory protein-1gamma. *Osteoarthritis Cartilage.* 2011; 19(6):728–736. [PubMed: 21376128]
32. Kawashiri SY, Kawakami A, Iwamoto N, Fujikawa K, Aramaki T, Tamai M, et al. Proinflammatory cytokines synergistically enhance the production of chemokine ligand 20 (CCL20) from rheumatoid fibroblast-like synovial cells in vitro and serum CCL20 is reduced in vivo by biologic disease-modifying antirheumatic drugs. *J Rheumatol.* 2009; 36(11):2397–2402. [PubMed: 19797510]
33. Flytlie HA, Hvid M, Lindgreen E, Kofod-Olsen E, Petersen EL, Jorgensen A, et al. Expression of MDC/CCL22 and its receptor CCR4 in rheumatoid arthritis, psoriatic arthritis and osteoarthritis. *Cytokine.* 2010; 49(1):24–29. [PubMed: 19942450]
34. Chabaud M, Page G, Miossec P. Enhancing effect of IL-1, IL-17, and TNF-alpha on macrophage inflammatory protein-3alpha production in rheumatoid arthritis: regulation by soluble receptors and Th2 cytokines. *J Immunol.* 2001; 167(10):6015–6020. [PubMed: 11698482]
35. Matsui T, Akahoshi T, Namai R, Hashimoto A, Kurihara Y, Rana M, et al. Selective recruitment of CCR6-expressing cells by increased production of MIP-3 alpha in rheumatoid arthritis. *Clin Exp Immunol.* 2001; 125(1):155–161. [PubMed: 11472439]
36. Nakayama T, Hieshima K, Nagakubo D, Sato E, Nakayama M, Kawa K, et al. Selective induction of Th2-attracting chemokines CCL17 and CCL22 in human B cells by latent membrane protein 1 of Epstein-Barr virus. *J Virol.* 2004; 78(4):1665–1674. [PubMed: 14747532]
37. Taub DD, Conlon K, Lloyd AR, Oppenheim JJ, Kelvin DJ. Preferential migration of activated CD4+ and CD8+ T cells in response to MIP-1 alpha and MIP-1 beta. *Science.* 1993; 260(5106): 355–358. [PubMed: 7682337]
38. Tak PP, Smeets TJ, Daha MR, Kluin PM, Meijers KA, Brand R, et al. Analysis of the synovial cell infiltrate in early rheumatoid synovial tissue in relation to local disease activity. *Arthritis Rheum.* 1997; 40(2):217–225. [PubMed: 9041933]
39. Torikai E, Kageyama Y, Suzuki M, Ichikawa T, Nagano A. The effect of infliximab on chemokines in patients with rheumatoid arthritis. *Clin Rheumatol.* 2007; 26(7):1088–1093. [PubMed: 17111092]
40. Kageyama Y, Ichikawa T, Nagafusa T, Torikai E, Shimazu M, Nagano A. Etanercept reduces the serum levels of interleukin-23 and macrophage inflammatory protein-3 alpha in patients with rheumatoid arthritis. *Rheumatol Int.* 2007; 28(2):137–143. [PubMed: 17619881]
41. Pickens SR, Chamberlain ND, Volin MV, Pope RM, Mandelin AM 2nd, Shahrara S. Characterization of CCL19 and CCL21 in rheumatoid arthritis. *Arthritis Rheum.* 2011; 63(4):914–922. [PubMed: 21225692]
42. Scanzello CR, McKeon B, Swaim BH, DiCarlo E, Asomugha EU, Kanda V, et al. Synovial inflammation in patients undergoing arthroscopic meniscectomy: Molecular characterization and relationship to symptoms. *Arthritis & Rheumatism.* 2011; 63(2):391–400. [PubMed: 21279996]
43. Elliott DM, Guilak F, Vail TP, Wang JY, Setton LA. Tensile properties of articular cartilage are altered by meniscectomy in a canine model of osteoarthritis. *J Orthop Res.* 1999; 17(4):503–508. [PubMed: 10459755]
44. Glasson SS, Blanchet TJ, Morris EA. The surgical destabilization of the medial meniscus (DMM) model of osteoarthritis in the 129/SvEv mouse. *Osteoarthritis Cartilage.* 2007; 15(9):1061–1069. [PubMed: 17470400]

45. Loeser RF, Olex AL, McNulty MA, Carlson CS, Callahan MF, Ferguson CM, et al. Microarray analysis reveals age-related differences in gene expression during the development of osteoarthritis in mice. *Arthritis Rheum.* 2012; 64(3):705–717. [PubMed: 21972019]
46. van Lent PL, Blom AB, Schelbergen RF, Sloetjes A, Lafeber FP, Lems WF, et al. Active involvement of alarmins S100A8 and S100A9 in the regulation of synovial activation and joint destruction during mouse and human osteoarthritis. *Arthritis Rheum.* 2012; 64(5):1466–1476. [PubMed: 22143922]
47. Chia SL, Sawaji Y, Burleigh A, McLean C, Inglis J, Saklatvala J, et al. Fibroblast growth factor 2 is an intrinsic chondroprotective agent that suppresses ADAMTS-5 and delays cartilage degradation in murine osteoarthritis. *Arthritis Rheum.* 2009; 60(7):2019–2027. [PubMed: 19565481]
48. Salminen H, Perala M, Lorenzo P, Saxne T, Heinegard D, Saamanen A, et al. Up-regulation of cartilage oligomeric matrix protein at the onset of articular cartilage degeneration in a transgenic mouse model of osteoarthritis. *Arthritis Rheum.* 2000; 43(8):1742–1748.
49. Tarrant TK, Liu P, Rampersad RR, Esserman D, Rothlein LR, Timoshchenko RG, et al. Decreased Th17 and antigen-specific humoral responses in CX(3) CR1-deficient mice in the collagen-induced arthritis model. *Arthritis Rheum.* 2012; 64(5):1379–1387. [PubMed: 22144035]
50. Bondeson J, Wainwright SD, Lauder S, Amos N, Hughes CE. The role of synovial macrophages and macrophage-produced cytokines in driving aggrecanases, matrix metalloproteinases, and other destructive and inflammatory responses in osteoarthritis. *Arthritis Res Ther.* 2006; 8(6):R187. [PubMed: 17177994]
51. Eisenberg SP, Evans RJ, Arend WP, Verderber E, Brewer MT, Hannum CH, et al. Primary structure and functional expression from complementary DNA of a human interleukin-1 receptor antagonist. *Nature.* 1990; 343(6256):341. [PubMed: 2137201]
52. Piguet PF, Grau GE, Vesin C, Loetscher H, Gentz R, Lesslauer W. Evolution of collagen arthritis in mice is arrested by treatment with anti-tumour necrosis factor (TNF) antibody or a recombinant soluble TNF receptor. *Immunology.* 1992; 77(4):510–514. [PubMed: 1337334]
53. Thorbecke GJ, Shah R, Leu CH, Kuruvilla AP, Hardison AM, Palladino MA. Involvement of Endogenous Tumor Necrosis Factor {alpha} and Transforming Growth Factor {beta} During Induction of Collagen Type II Arthritis in Mice. *PNAS.* 1992; 89(16):7375–7379. [PubMed: 1502148]
54. Williams RO, Feldmann M, Maini RN. Anti-Tumor Necrosis Factor Ameliorates Joint Disease in Murine Collagen- Induced Arthritis. *PNAS.* 1992; 89(20):9784–9788. [PubMed: 1409699]
55. Bakker AC, Joosten LA, Arntz OJ, Helsen MM, Bendele AM, van de Loo FA, et al. Prevention of murine collagen-induced arthritis in the knee and ipsilateral paw by local expression of human interleukin-1 receptor antagonist protein in the knee. *Arthritis Rheum.* 1997; 40(5):893–900. [PubMed: 9153551]

**Figure 1.**

Gene expression and serum levels of cytokines in C57BL/6 and MRL/MpJ mice following fracture. **(A)** RT-PCR data showing relative change of gene expression in synovial tissue from C57BL/6 mice (black bars) and MRL/MpJ mice (light bars) ($n=6$ for each strain) following fracture (fx). Greater than 3-fold change in expression was considered significant. **(B)** IL-1 α ELISA of serum samples from C57BL/6 (black circles) and MRL/MpJ (light diamonds) mice following fracture. **(C)** IL-1 β ELISA of serum samples. Data in **B,C** are presented as mean \pm SD; § indicates significant differences between C57BL/6 and MRL/MpJ mice at each time point (Mann-U Whitney, $p<0.05$); # indicates significant differences with time post-fracture within a mouse strain (Kruskal-Wallis, $p<0.04$).

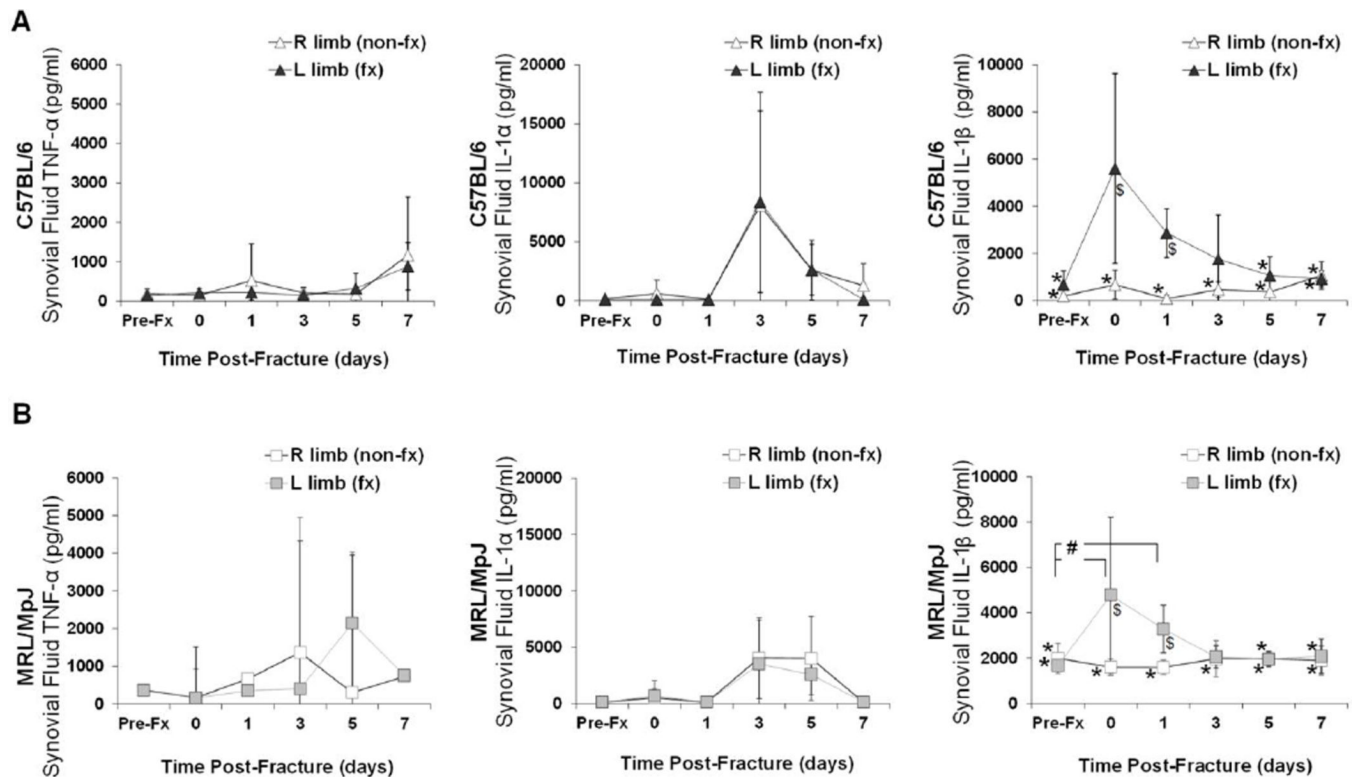
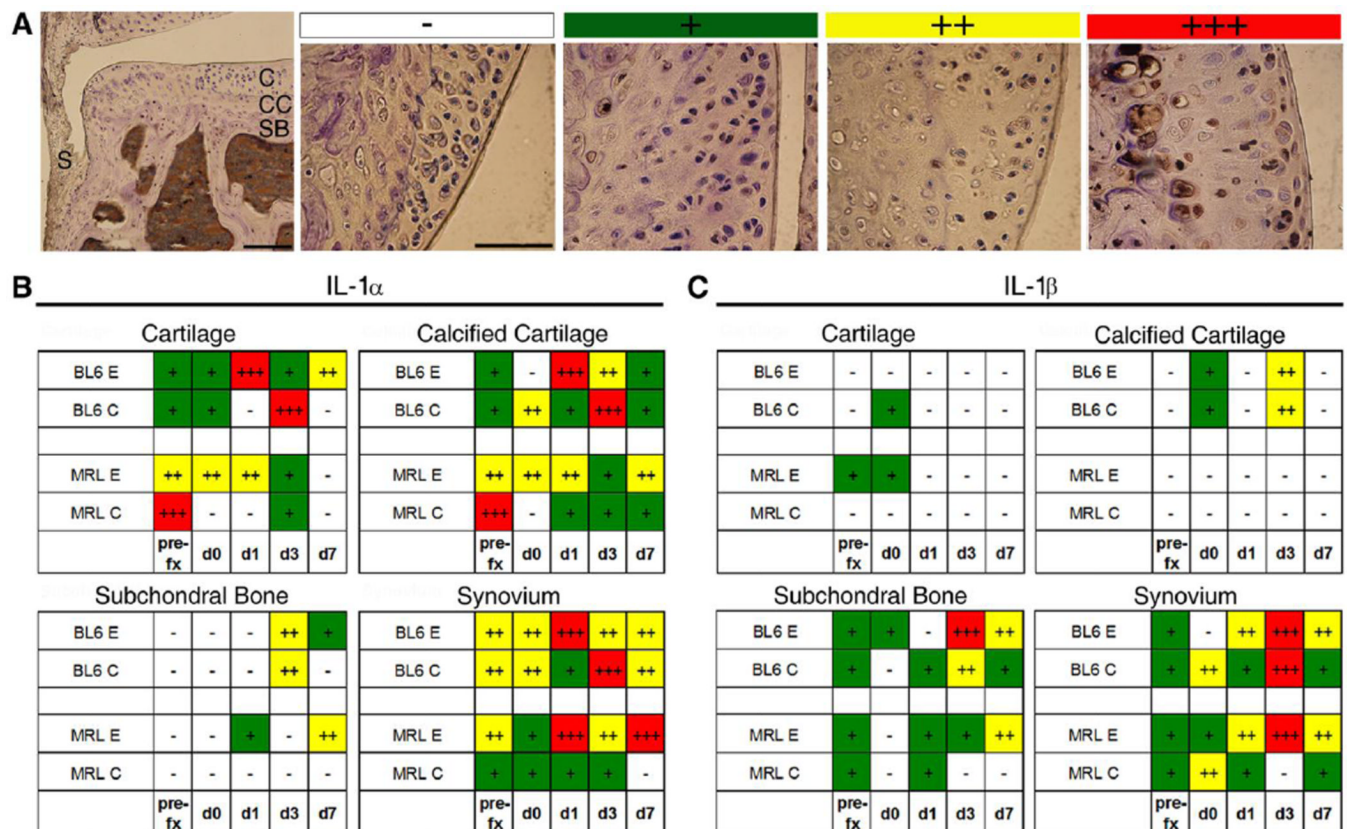


Figure 2.

Synovial fluid concentrations of TNF- α , IL-1 α and IL-1 β in (A) C57BL/6 mice and (B) MRL/MpJ mice following fracture. TNF- α , IL-1 α , and IL-1 β ELISA of synovial fluid samples from fractured (closed shapes) and non-fractured (open shapes) limbs following fracture. Data presented as mean \pm SD; \$ indicates significant differences between fractured and non-fractured limbs (Wilcoxon matched pairs test, $p < 0.03$); * indicates significant differences between C57BL/6 and MRL/MpJ mice at each time point for fractured and non-fractured limbs independently (Mann-U Whitney, $p < 0.03$); # indicates significant differences with time post-fracture within a mouse strain (Kruskal-Wallis, $p < 0.02$).

**Figure 3.**

Qualitative assessment of immunohistochemistry for IL-1. (A) Regions graded included the synovium (S), articular cartilage (C), calcified cartilage (CC), and subchondral bone (SB). Staining intensity in all four regions of the joint was discretely graded on a four-point qualitative scale, (-) to (+++), with (-) indicating minimal staining and (+++) indicating maximal staining. (B) IL-1 α staining observed in C57BL/6 fractured (BL6 E), C57BL/6 non-fractured (BL6 C), MRL/MpJ fractured (MRL E) and MRL/MpJ non-fractured (MRL C) limbs (n=6 of each). (C) IL-1 β staining as observed in the same limbs as in B. Scale bars are 100 μ m, fx=fracture, and d=days post-fracture.

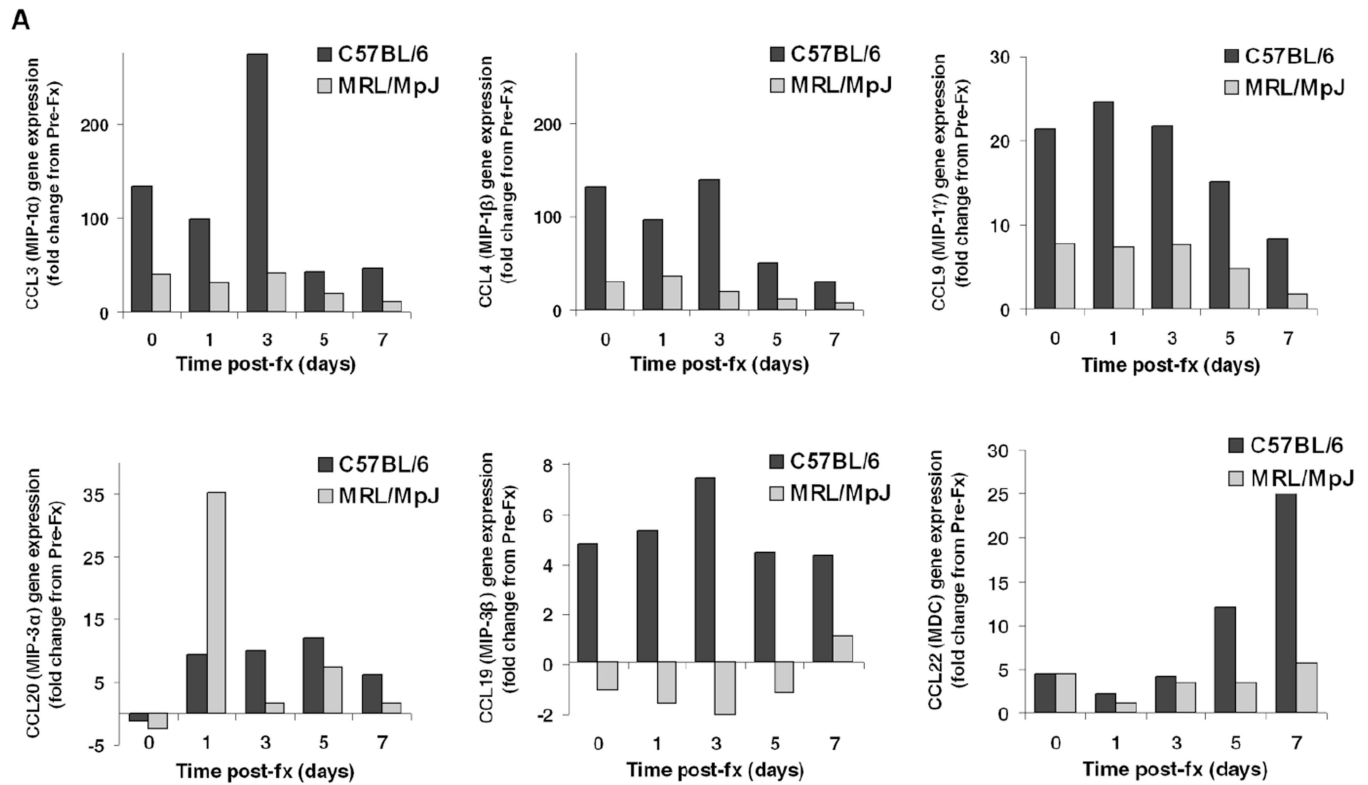


Figure 4.

Increased expression of macrophage-associated chemokines in C57BL/6 versus MRL/MpJ mice following articular fracture. RT-PCR data showing relative change of gene expression in synovial tissue from C57BL/6 mice (black bars) and MRL/MpJ mice (light bars) (n=6 for each strain) following fracture. Greater than 3-fold change in expression was considered significant.

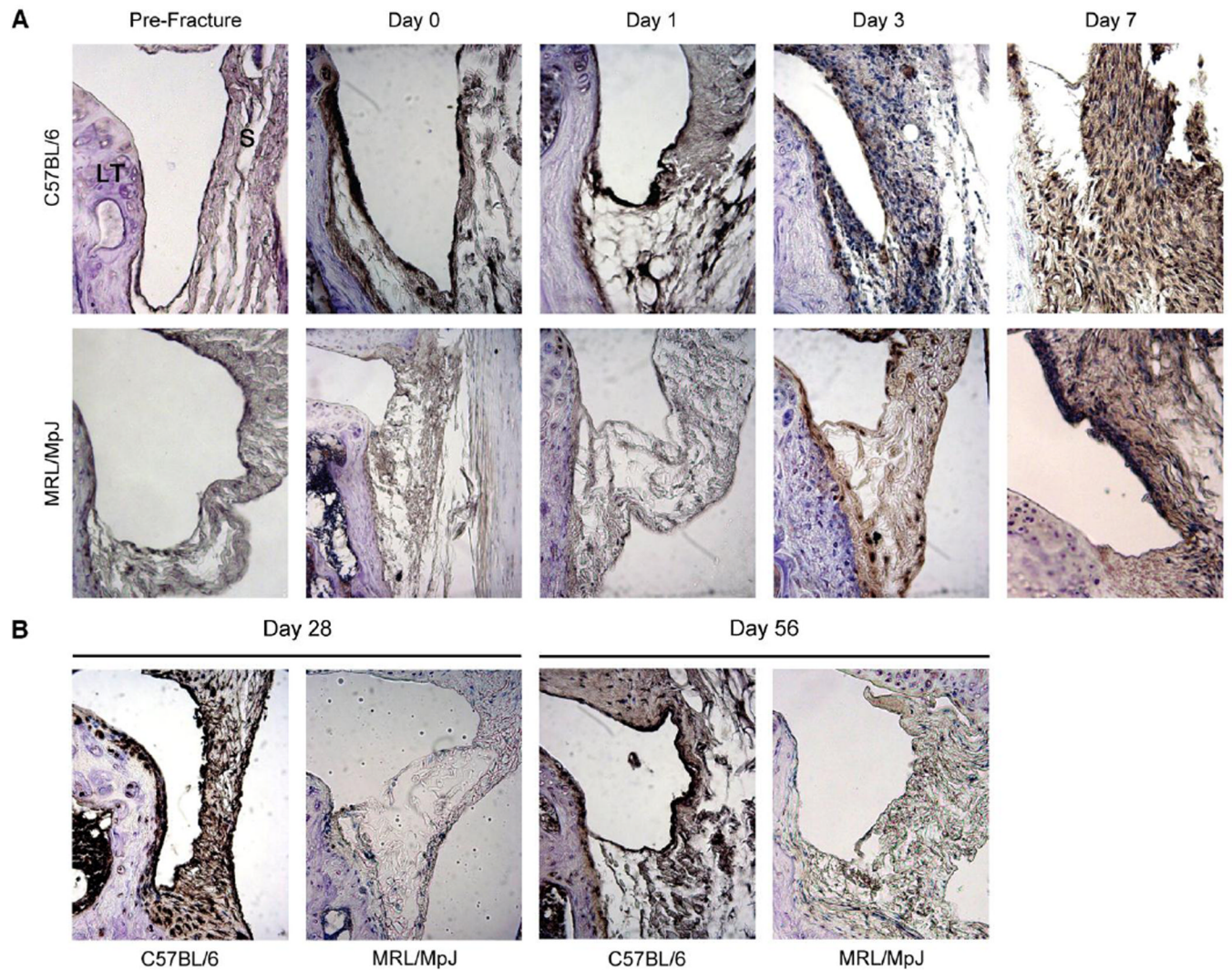


Figure 5.

Increased synovial macrophage infiltration in C57BL/6 versus MRL/MpJ mice following intra-articular fracture. **(A)** Macrophage immunohistochemistry (F4/80 staining) in the lateral synovium of fractured limbs in the first week after fracture. **(B)** Macrophage IHC at 28 and 56 days after fracture. LT= lateral tibia, S=synovium, brown = positive IHC stain, blue = hematoxylin counterstain; 400× magnification.

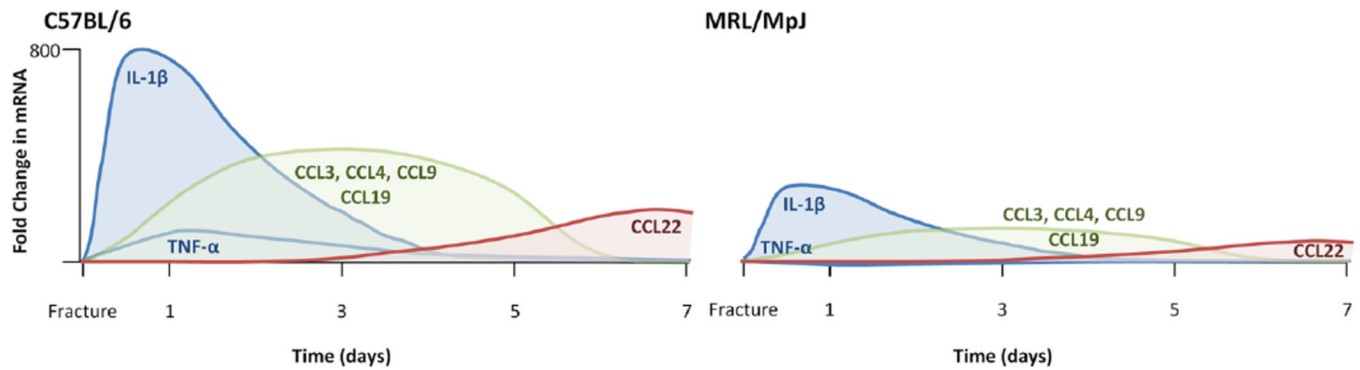


Figure 6.

Timeline of increased inflammatory response for C57BL/6 compared to MRL/MpJ mice following joint injury. Schematic of relative gene expression of cytokines, IL-1 β and TNF- α (in blue), were elevated first, followed by an elevation in chemokine gene expression for CCL3, CCL4, CCL9 and CCL19, the macrophage inflammatory proteins (in green), and lastly with an increase in gene expression of macrophage derived chemokine, CCL22 (in red).